

# Correlation between Crystal and Electronic Structures in Diketopyrrolopyrrole Pigments as Viewed from Exciton Coupling Effects

Jin Mizuguchi

Faculty of Engineering, Yokohama National University, 79-5 Tokiwadai, Hodogaya-ku, 240-8501 Yokohama, Japan

Received: July 7, 1999; In Final Form: December 28, 1999

Diketopyrrolopyrroles (DPPs) are industrially important red pigments. The color in the solid state changes variously from vivid red to yellowish red, although no noticeable difference is recognized in the molecular spectra in solution. The correlation between the electronic and crystal structures of some DPP pigments has been investigated on the basis of the exciton coupling effects. The polarized reflection spectra on these single crystals revealed that the reflection maximum is hypsochromically shifted as the extent of molecular overlap along the stacking axis is increased. We assumed the present color change as arising from interactions between transition moments and calculated the spectral shifts for the nearest-neighbor molecules. The hydrogen-bond pair (“head-to-tail” arrangement) is found to displace the absorption maximum toward longer wavelengths, while the stack pair (“parallel” arrangement) significantly contributes to the hypsochromic shift. The present result is qualitatively in good agreement with the experiment.

## 1. Introduction

Diketopyrrolopyrroles (abbreviated to DPPs; shown in Figure 1)<sup>1</sup> are industrially important red pigments side by side with phthalocyanine, quinacridone, and perylene pigments.<sup>2</sup> DPPs belong to the class of hydrogen-bonded pigments such as quinacridone and indigo compounds.<sup>2</sup> One of the appealing features of the H-bond pigments is to exhibit vivid red or blue colors in the solid state, although their molecular weights are quite small (DPP = 288, quinacridone = 292, and indigo = 262) and they are thus vaguely colored in solution. The H-bond pigments are typically composed of a  $\pi$ -conjugated system as chromophore and of two pairs of NH (donor) and C=O (acceptor) as auxochromes. The molecules are firmly held together in the solid state by means of intermolecular hydrogen bonds based on NH $\cdots$ O, forming a three-dimensional H-bond network.

DPP derivatives shown in Figure 1 exhibit a variety of shades in the solid state, although no significant difference is recognized in solution spectra.<sup>3,4</sup> For example, *p*-Cl(DPP) shows a vivid red, while *m*-CN(DPP) bears yellowish red. Roughly speaking, the yellowish component increases in single crystals from *p*-Cl(DPP) (left) via DPP (middle) to *m*-CN(DPP) (right). A series of investigations on the crystal and electronic structures have been carried out on DPP, *p*-Cl(DPP), and *m*-Cl(DPP).<sup>3–6</sup> Quite recently, the crystal structures of TB–DPP<sup>7</sup> and *m*-CN(DPP)<sup>8</sup> have also been reported. These investigations so far can be summarized as follows: (1) The intermolecular hydrogen bond based on NH $\cdots$ O is effective in displacing the absorption maximum toward longer wavelengths upon crystallization by an amount of about 1500 cm<sup>-1</sup>. (2) The spectral shape of the solid-state spectra is quite different, depending on the extent of the molecular overlap along the stacking axis. For example, the solid-state spectrum is quite similar to the solution spectrum when the molecular overlap is insignificant. On the other hand, the absorption maximum is more displaced toward shorter wavelengths with the increase of molecular overlap, making the color more yellowish.

Despite the above experimental findings, the detailed mechanism of the different shades remains unclarified. For this reason, an attempt was made to elucidate the mechanism in terms of intermolecular interactions between transition dipoles (“exciton coupling effects”). We calculated the spectral shifts for five different DPPs on the basis of the crystal structure and found the result consistent with the experiment.

## 2. Crystal Structures of DPP Pigments

Table 1 summarizes the crystallographic parameters for DPP,<sup>5</sup> *p*-Cl(DPP) and *m*-Cl(DPP),<sup>6</sup> TB–DPP,<sup>7</sup> and *m*-CN(DPP).<sup>8</sup> All DPP pigments except for *p*-Cl(DPP) belong to the triclinic crystal system, and the molecules are arranged in a fashion *quasi* “bricks in a brick wall”. The structure of *m*-CN(DPP) is found isomorphous with that of *m*-Cl(DPP). On the other hand, in TB–DPP, the molecular symmetry is reduced from  $C_i$  to  $C_1$  upon crystallization, producing a dipole moment of about 0.3 D. In addition, the two phenyl rings are twisted in the opposite direction and the torsion angle is also different, whereas in other DPPs the twisting of the phenyl rings takes place in the same direction as characterized by the  $C_i$  symmetry. Furthermore, the heterocyclic ring system is not planar in TB–DPP but slightly folded in the middle by about 3°, while it is completely planar in other DPPs.

Figure 2 shows the projection of the crystal structure of DPP onto the (*b*,*c*) and (*a*,*c*) planes.<sup>4,5</sup> There are four intermolecular hydrogen bonds per molecule between the NH group of one molecule and the O atom of the neighboring one along the *b* axis. The present H-bond network is formed in common in all DPP pigments, but the molecular overlap along the stacking axis is quite different for each DPP derivative. Figure 3 illustrates the typical overlap of two molecules for *p*-Cl(DPP) and *m*-Cl(DPP). The number of atomic contacts along the stacking axis as designated by dotted ellipses is 2, 6, 9, 12, and 15 for *p*-Cl(DPP),<sup>6</sup> TB–DPP,<sup>7</sup> DPP,<sup>5</sup> *m*-Cl(DPP),<sup>6</sup> and *m*-CN(DPP),<sup>8</sup> respectively. The extent of the overlap increases from

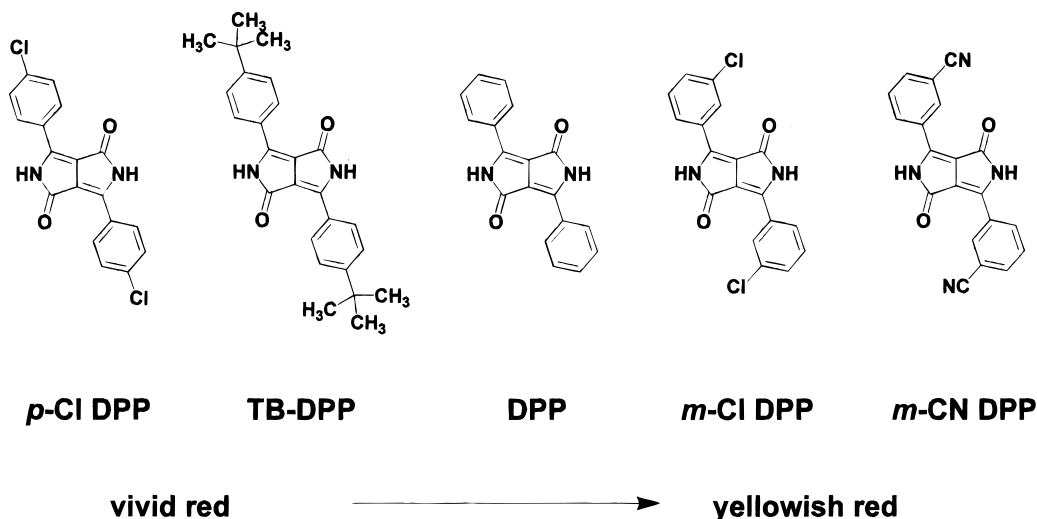


**Figure 1.** Molecular structures of DPP derivatives.

**TABLE 1: Crystallographic Parameters for DPP Pigments**

	DPP <sup>5</sup>	TB-DPP <sup>7</sup>	<i>p</i> -Cl(DPP) <sup>6</sup>	<i>m</i> -Cl(DPP) <sup>6</sup>	<i>m</i> -CN(DPP) <sup>8</sup>
molecular symmetry	$C_i$	$C_1$	$C_i$	$C_i$	$C_i$
<i>Z</i>	1	2	2	1	1
space group	$P\bar{1}$	$P\bar{1}$	$P2_1/n$	$P\bar{1}$	$P\bar{1}$
lattice constants					
<i>a</i> (Å)	3.817(1)	7.229(1)	5.658(1)	3.785(1)	6.841(4)
<i>b</i> (Å)	6.516(1)	9.872(1)	23.099(3)	6.845(1)	14.801(4)
<i>c</i> (Å)	13.531(2)	15.779(1)	5.585(1)	14.485(2)	3.734(4)
$\beta$ (°)	86.97(1)	96.31(1)	99.07(1)	97.60(1)	97.85(6)
<i>V</i> (Å <sup>3</sup> )	334.3(2)	1108.9	720.8(4)	362.0(2)	371.3(5)
torsion angle of the phenyl ring, deg	7(1) in the same direction	4.9/8.0 in opposite directions	3(2) in the same direction	10.3(3) in the same direction	10.0(2) in the same direction
dihedral angle, deg	180	176.6	180	180	180
molecular stacking	pseudobricks in a brick wall	bricks in a brick wall	herringbone	pseudobricks in a brick wall	pseudobricks in a brick wall
dipole moment, <sup>a</sup> D	0	0.36	0	0	0

<sup>a</sup> Determined by MOPAC93.

*p*-Cl(DPP) via DPP to *m*-CN(DPP) (Figure 1) and is in line with the increasing order of yellowish component.

### 3. Observed Correlation between Spectral Shape and Molecular Overlap in the Solid State<sup>4</sup>

Figure 4 shows the three characteristic spectra of evaporated DPP measured at room temperature. Spectrum a is obtained as evaporated, and its spectral shape is quite similar to that in solution ( $\lambda_{\max} = 507$  nm). Spectrum a is then transformed via b into c when exposed to the vapor of certain organic solvents such as acetone. Spectra a, b, and c represent the spectral shapes of the polarized reflection spectra of DPP single crystals: spectrum a corresponds to the spectral of *p*-Cl(DPP) ( $\lambda_{\max} = 550$  nm) and TB-DPP ( $\lambda_{\max} = 531$  nm), spectrum b to DPP ( $\lambda_{\max} = 459$  nm), and spectrum c to *m*-Cl(DPP) ( $\lambda_{\max} = 450$  nm) and *m*-CN(DPP) ( $\lambda_{\max} = 444$  nm).

The evaporated DPP film before vapor treatment is found to be crystallized as shown in Figure 5. The molecules are clearly ordered along the (001) direction (van der Waals interactions) but little ordered along the (1,1,1) direction (stacking axis). The present phase is also characterized by NH $\cdots$ O intermolecular hydrogen bonds as confirmed by IR spectra. So the spectral displacement on going from solution to the solid state (507  $\rightarrow$  540 nm) is found to arise from the intermolecular hydrogen bonds. On the other hand, vapor treatment brings about the ordering of the molecules along the stacking (1,1,1) axis (Figure

5). This result evidently indicates that the absorption maximum is displaced toward shorter wavelengths as the molecules are ordered along the stacking axis.

### 4. Exciton Coupling Effects and Spectral Shifts

**4.1. Outline of the Calculation.** When a photoexcitation induces a transition dipole in the molecule, the excited state in crystals involves wave functions with significant probabilities on the nearest neighbors. Therefore, the exciton coupling may well involve energy contributions from interactions with all of these nearest-neighbor molecules acting in concert in the lattice. This may lead to the band splitting of the excited state ("Davydov splitting") or displace the excited energy level downward (red shift) or upward (blue shift), depending on the relative orientation of the transition dipoles: "head-to-tail" or "parallel".

The exciton displacement energy ( $\Delta E_{\text{exciton}}$ ) is given by the following dipole-dipole equation:<sup>9-11</sup>  $\Delta E_{\text{exciton}} = |\mu|^2(1 - 3\cos^2\theta)/r^3$ , where the transition dipole is denoted by  $\mu$  and the distance and angle between two transition dipoles by  $r$  and  $\theta$ , respectively. The term  $(1 - 3\cos^2\theta)/r^3$  determines the geometrical relationship of transition dipoles which is related to the crystal structure. Since the transition dipole (i.e., absorption coefficient) is quite large in dyes and pigments, the exciton coupling (i.e., interneighbor coupling) plays an important role to displace absorption bands in the solid state.

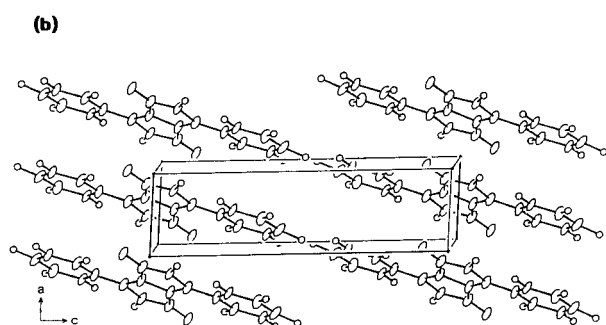
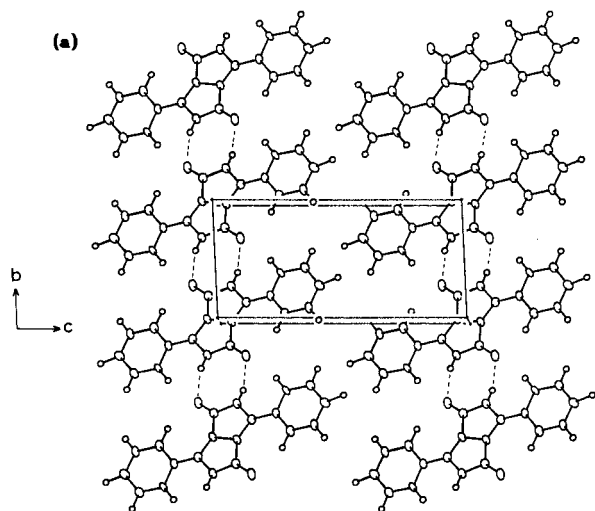


**Figure 2.** Projection of the crystal structure of DPP: (a) onto (*b,c*) plane and (b) (*a,c*) plane.

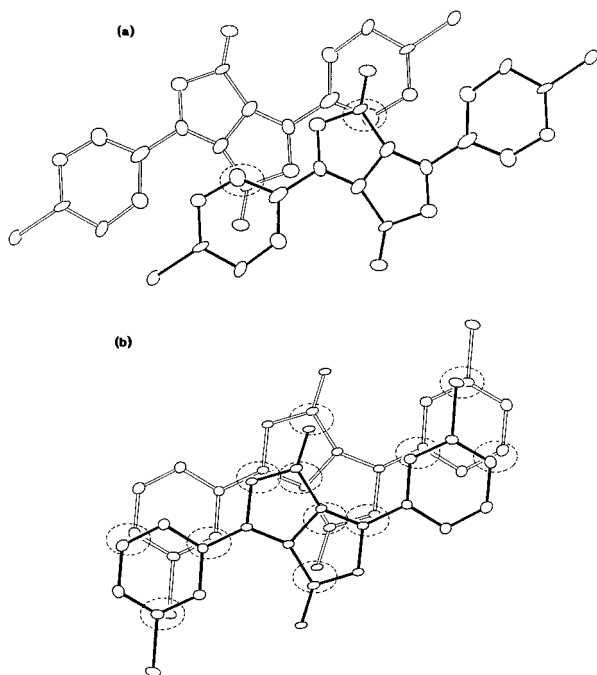


**Figure 3.** Overlap of two molecules for *p*-Cl(DPP) and *m*-Cl(DPP). The directly overlapping atoms are designated by ellipses.

The transition energy for a molecule pair ( $\Delta E_{\text{pair}}$ ) in the solid state is given by the following equation:<sup>9-11</sup>

$$\Delta E_{\text{pair}} = \Delta E_{\text{monomer}} + \Delta D \pm \Delta E_{\text{exciton}}$$

where  $\Delta E_{\text{monomer}}$  stands for the electronic transition energy for

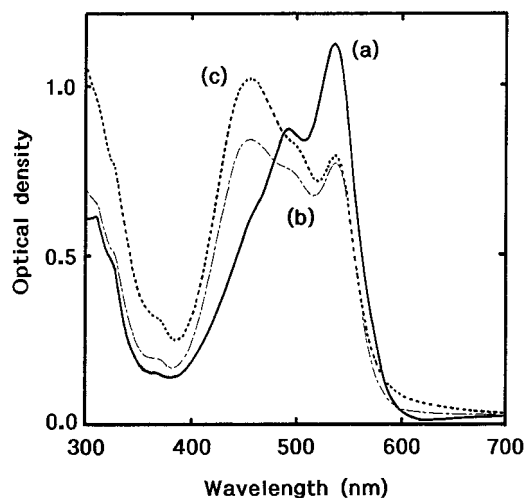


**Figure 4.** Spectral change of evaporated DPP due to vapor treatment. The yellowish component increases from spectrum a via b to c.

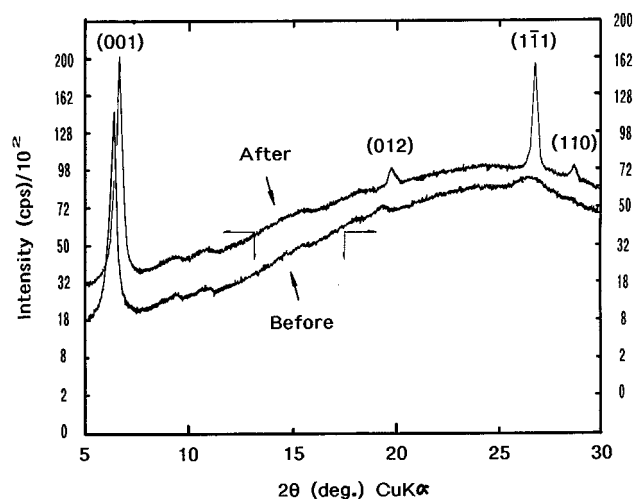


**Figure 5.** X-ray diffraction diagrams of evaporated DPP: (a) before and (b) after vapor treatment.

the component molecule and  $\Delta D$  is the stabilization energy as obtained by subtraction of the “van der Waals” energy in the ground state from that in the excited state. This term is called the “crystal shift” upon crystallization due to the polarization effect.  $\Delta E_{\text{exciton}}$  denotes the exciton displacement energy which will be evaluated in the following.

The exciton coupling treatment has variously been employed in the interpretation of the absorption spectra in molecular crystals or dye aggregates: anthracene, perylene, naphthalene, and tetracene,<sup>10-11</sup> J-aggregates of cyanine dyestuffs,<sup>12</sup> thionated DPP,<sup>13</sup> black perylene pigment,<sup>14</sup> and magnesium phthalocyanine complexes.<sup>15</sup>

In the present investigation, the exciton displacement energies have been calculated for the nearest molecule pairs of DPP derivatives, since the exciton displacement energy described above falls off as the inverse cube of distance so that most of the interaction would come from the nearest neighbors as confirmed by our previous investigations.<sup>13-15</sup>  $\mu$  is first calculated from the *xyz* coordinate sets of X-ray structures<sup>5-8</sup> on the basis of the INDO/S Hamiltonian.<sup>16</sup> The result is given as transition dipole lengths in Tables 2-4. The transition dipole is known to point to the direction of the intermolecular hydrogen bond as determined by polarized reflection spectra on single crystals.<sup>4</sup> The distance  $r$  and angle  $\theta$  are taken from the crystal structure

**TABLE 2: Spectral Shift Due to Exciton Coupling Effects for *p*-Cl(DPP): 12 Nearest Neighbors around the Molecule at  $(\frac{1}{2}, \frac{1}{2}, 0)$** 

type of molecule pairs	no. of equiv molecules	site	$r, \text{\AA}$	$\theta, \text{deg}$	$\Delta E^a, \text{cm}^{-1}$
<b>hydrogen bond pair</b>	2	$(\frac{3}{2}, \frac{1}{2}, 1)$	<b>7.297</b>	<b>3.460</b>	<b>-2116<sup>b</sup></b>
stack pair I	2	$(\frac{1}{2}, \frac{1}{2}, 1)$	5.585	49.047	-731
stack pair II	2	$(\frac{3}{2}, \frac{1}{2}, 0)$	5.658	48.208	-809
stack pair III	2	$(\frac{3}{2}, \frac{1}{2}, -1)$	8.425	89.252	734
diagonal pair	4	$(1, 0, \frac{1}{2})$	12.135	68.330	148
total	12				<b>-5252</b>

<sup>a</sup>  $\mu (\text{\AA}) = 1.9462$ . <sup>b</sup> The minus or plus sign denotes the hypsochromic or bathochromic shift, respectively.

**TABLE 3: Spectral Shift Due to Exciton Coupling Effects for DPP: 14 Nearest Neighbors around the Molecule at  $(\frac{1}{2}, 0, 0)$** 

type of molecule pairs	no. of equiv molecules	site	$r, \text{\AA}$	$\theta, \text{deg}$	$\Delta E^a, \text{cm}^{-1}$
<b>hydrogen bond pair</b>	2	$(\frac{3}{2}, 1, 0)$	<b>7.258</b>	<b>3.1</b>	<b>-1899<sup>b</sup></b>
<b>stack pair along the <i>a</i> axis</b>	2	$(\frac{3}{2}, 0, 0)$	<b>3.817</b>	<b>66.7</b>	<b>3474</b>
diagonal pair I	2	$(\frac{1}{2}, 1, 1)$	14.696	66.5	60
diagonal pair II	1	$(\frac{3}{2}, 2, 1)$	18.577	45.1	-20
diagonal pair III	1	$(\frac{1}{2}, 0, 1)$	13.864	84.3	133
diagonal pair IV	2	$(\frac{3}{2}, 0, 1)$	14.252	83.4	121
<b>diagonal pair I along the H-bond pair</b>	2	$(\frac{1}{2}, 1, 0)$	<b>6.516</b>	<b>28.4</b>	<b>-1746</b>
diagonal pair II	2	$(\frac{3}{2}, 1, 1)$	15.220	61.0	31
total	14				<b>195</b>

<sup>a</sup>  $\mu (\text{\AA}) = 1.984$ . <sup>b</sup> The minus or plus sign denotes the hypsochromic or bathochromic shift, respectively.

**TABLE 4: Spectral Shift Due to Exciton Coupling Effects for *m*-Cl(DPP): 14 Nearest Neighbors around the Molecule at  $(\frac{1}{2}, 1, 0)$** 

type of molecule pairs	no. of equivalent molecules	site	$r, \text{\AA}$	$\theta, \text{deg}$	$\Delta E^a, \text{cm}^{-1}$
<b>hydrogen bond pair</b>	2	$(\frac{3}{2}, 0, 0)$	<b>7.280</b>	<b>3.3</b>	<b>-1928<sup>b</sup></b>
<b>stack pair along the <i>a</i> axis</b>	2	$(\frac{3}{2}, 1, 0)$	<b>3.785</b>	<b>71.1</b>	<b>4713</b>
diagonal pair I	1	$(\frac{3}{2}, 2, 1)$	15.498	70.5	67
diagonal pair II	1	$(\frac{1}{2}, 0, 1)$	17.140	61.7	24
diagonal pair III	2	$(\frac{3}{2}, 0, 1)$	16.895	50.3	-17
diagonal pair IV	2	$(\frac{3}{2}, 0, 1)$	14.252	83.4	-26
<b>diagonal pair I along the H-bond pair</b>	2	$(\frac{1}{2}, 0, 0)$	<b>6.845</b>	<b>28.4</b>	<b>-1559</b>
diagonal pair II	2	$(\frac{3}{2}, 0, 0)$	9.369	25.0	-667
total	14				<b>1123</b>

<sup>a</sup>  $\mu (\text{\AA}) = 1.798$ . <sup>b</sup> The minus or plus sign denotes the hypsochromic or bathochromic shift, respectively.

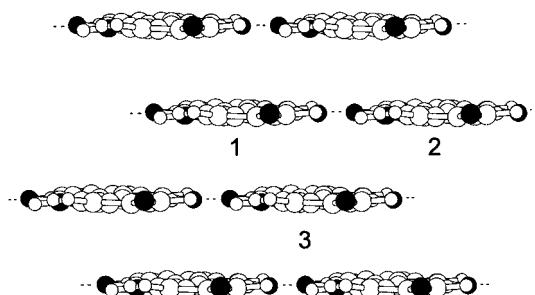


**Figure 6.** Molecular arrangement of *p*-Cl(DPP). The intermolecular H bonds are present along the horizontal direction and designated by dotted lines.

for five DPPs.<sup>5-8</sup> Finally, each energy contribution is summed up in consideration of the number of equivalent molecules.

**4.2. Results and Discussion.** Figure 6 shows the molecular stack of *p*-Cl(DPP) as viewed from the long molecular axis. The intermolecular hydrogen bonds are present on the horizontal plane between the NH group of molecule 1 and the O atom of molecule 2. The energy calculation has been made for the nearest-neighbor molecules around molecule 1. The combination of molecules 1 and 2 is a hydrogen bond pair. There are two kinds of stack pairs: one is a less-overlapped pair composed of molecules 2 and 3, and the other is a more-overlapped pair consisting of molecules 1 and 3. The calculated results are shown in Table 2.

The largest contribution to the bathochromic shift is made by the H-bond pair ( $-2100 \text{ cm}^{-1}$ ), since the angle is very small

and the distance is relatively short. The additional contribution is found in stack pairs I and II by amounts of  $-731$  and  $-809 \text{ cm}^{-1}$ , respectively, where the angles are slightly smaller than  $54.7^\circ$ . On the other hand, the hypsochromic component is given by stack pair III and the cross pair whose angles are larger than  $54.7^\circ$ . The total shift energy amounts to  $-5252 \text{ cm}^{-1}$ . The present result indicates that the bathochromic shift prevails due to the H-bond pair, while the hypsochromic component is small because of the lack of atomic contacts along the stacking axis. The hypsochromic component, however, tends to increase significantly from *p*-Cl(DPP) via DPP to *m*-CN(DPP) due to the increased number of atomic contacts.

Next, we examine the cases for DPP and *m*-Cl(DPP), where there are 9 and 12 atomic contacts along the molecular stack, respectively. The results are shown in Tables 3 and 4, respectively. The energy shift for the H-bond pair is calculated to be about  $-1900 \text{ cm}^{-1}$  in common for DPP pigments. On the other hand, the hypsochromic contribution due to stack pairs is remarkable in DPP and particularly in *m*-Cl(DPP). The hypsochromic contribution slightly exceeds in DPP and greatly exceeds in *m*-Cl(DPP). The extent of the hypsochromic displacement is again found to increase as the atomic contacts along the molecular stack become more significant.

Table 5 summarizes the calculated results for all DPP pigments. The extent of the hypsochromic displacement is clearly in line with the increased number of the atomic contacts along the stacking axis. The tendency of the spectral shift (signs and the orders of magnitude) is in fairly good agreement with

**TABLE 5: Calculated and Observed Spectral Shifts for DPP Pigments**

	calcd, cm <sup>-1</sup>	obsd, cm <sup>-1</sup>
<i>p</i> -Cl(DPP)	-5252	-1182
TB-DPP	-3214	-719
DPP	195	2086
<i>m</i> -Cl(DPP)	1123	2336
<i>m</i> -CN(DPP)	2801	3067

the experiment. In this sense, one can say that a spectroscopically parametrized semiempirical Hamiltonian (INDO/S) and a simple, ordered overlap model (i.e., a geometric model) combine to give rough qualitative agreement with the measured values of the spectral shifts.

However, the quantitative correlation is rather poor. There are several possible causes: (1) only the exciton displacement term ( $\Delta E_{\text{exciton}}$ ) was evaluated in the present calculation, excluding the contribution from the crystal shift ( $\Delta D$ ); (2) only the dipole-dipole interaction potential term in the multipole expansion of the intermolecular Coulomb potential was kept in the present calculation for the exciton coupling, neglecting higher potential terms; (3) energy contributions from the second nearest neighbors as well as the dielectric constants should be considered for the calculation. None of these is so simple to allow us to make reasonable estimations at the present stage of the investigation. Nevertheless, the author believes that the insight in terms of exciton coupling is valuable and serves as a good start for a color generation mechanism of dyes and pigments.

## 5. Conclusions

The spectral shifts for five kinds of DPP pigments have been calculated considering exciton coupling effects. The conclusions can be summarized as follows.

The H-bond pair shifts the absorption maximum toward longer wavelengths by about 2000 cm<sup>-1</sup>. On the contrary, the

stack pair contributes to the hypsochromic displacement by about 3000–4500 cm<sup>-1</sup>.

In *p*-Cl(DPP) and TB-DPP, the bathochromic contribution due to the H bond exceeds the hypsochromic contribution caused by stack pairs. On the other hand, in DPP, *m*-Cl(DPP), and *m*-CN(DPP), the stack pair contribution is larger than the H-bond contribution, leading to the hypsochromic shift.

The exciton coupling model based on the interaction between transition dipoles allows us to qualitatively interpret the correlation between the crystal and electronic structures in DPP pigments.

## References and Notes

- (1) Iqbal, A.; Cassar, L.; Rochat, A. C.; Phénninger, J.; Wallquist, O. *J. Coat. Technol.* **1988**, *60*, 37.
- (2) Herbst, W.; Hunger, K. *Industrial Organic Pigments*; VCH: Weinheim, New York, Basel, Cambridge, 1993.
- (3) Mizuguchi, J.; Wooden, G. *Ber. Bunsen-Ges. Phys. Chem.* **1991**, *95*, 1264.
- (4) Mizuguchi, J.; Rihs, G. *Ber. Bunsen-Ges. Phys. Chem.* **1992**, *96*, 597.
- (5) Mizuguchi, J.; Grubenmann, A.; Wooden, G.; Rihs, G. *Acta Crystallogr.* **1992**, *B48*, 696.
- (6) Mizuguchi, J.; Grubenmann, A.; Rihs, G. *Acta Crystallogr.* **1993**, *B49*, 1056.
- (7) Mizuguchi, J. *Acta Crystallogr.* **1998**, *C54*, 1482.
- (8) Mizuguchi, J.; Matsumoto, S. *Z. Kristallogr.-New Crystal Structures* **2000**, *215*, 195.
- (9) Kasha, M. *Spectroscopy of the Excited State*; Plenum Press: New York, 1976; p 337.
- (10) Craig, D. P.; Walmsley, S. H. *Excitons in Molecular Crystals*; W. A. Benjamin: New York, 1968.
- (11) Hochstrasser, R. M. *Molecular Aspects of Symmetry*; W. A. Benjamin: New York, Amsterdam, 1966.
- (12) Kobayashi, T. *J-aggregates*; World Scientific: Singapore, New Jersey, London, Hong Kong, 1996.
- (13) Mizuguchi, J. *Electrophotography* **1998**, *37*, 58.
- (14) Mizuguchi, J. *J. Appl. Phys.* **1998**, *84*, 4479.
- (15) Endo, A.; Matsumoto, S.; Mizuguchi, J. *J. Phys. Chem. A* **1999**, *103*, 8193.
- (16) Zerner, M. C. *ZINDO, A General Semiempirical Program Package*; Department of Chemistry, University of Florida: Gainesville, 32611.